Eur. Phys. J. B **18**, 23–30 (2000)

THE EUROPEAN PHYSICAL JOURNAL B

EDP Sciences
© Società Italiana di Fisica
Springer-Verlag 2000

Whole diffraction pattern-fitting of polycrystalline fcc materials based on microstructure

P. Scardi[a], M. Leoni, and Y.H. Dong

Dipartimento di Ingegneria dei Materiali, Università di Trento, 38050 Mesiano (TN), Italy

Received 16 May 2000

Abstract. A method is proposed for modelling the complete diffraction pattern of fcc polycrystalline materials. The algorithm permits a simultaneous refinement of several parameters related to microstructure and lattice defects responsible for line broadening effects. Linear (dislocations) and planar (stacking faults) defects are considered in detail, together with the effect of size and shape of coherent scattering domains (crystallites). Experimentally observed profiles are modelled by Voigt functions, whose parameters are connected with those describing the dislocation field (dislocation density, outer cut-off radius, average contrast factor), twin and deformation fault probabilities, and domain size, also considering the effect of a symmetrical instrumental profile. Domain shape is assumed spherical, with a lognormal distribution of diameters; however, the approach can be generalised to different shapes and size distributions. The proposed algorithm can be extended to other crystalline structures, and can be used within the Rietveld method or as a Whole Powder Pattern Fitting (WPPF), as in the present work.

PACS. 61.72.Dd Experimental determination of defects by diffraction and scattering – 61.72.Lk Linear defects: dislocations, disclinations – 61.72.Nn Stacking faults and other planar or extended defects

1 Introduction

In the recent years, analytical methods for the processing of diffraction data from polycrystalline materials developed in the direction of whole powder pattern fitting, *i.e.*, simultaneous analysis of an extended portion of the experimental pattern containing several diffraction profiles. This new paradigm in the powder diffraction research led to considerable benefits in two main areas: (a) structure solution and refinement from powder data and (b) study of the microstructure and lattice defects in polycrystalline materials. While (a) is of direct interest in crystallography and structural studies [1], (b) is a promising development in materials science [2,3], and is the direct object of the present study.

WPPF methods are used to determine (i) phase percentages in powder mixtures [4], (ii) lattice parameters [5], (iii) nature and concentration of line and plane defects [2,3], (iv) crystalline domain size and shape [3,6] and (v) texture [7]. Many existing WPPF computer programs are based on the Rietveld algorithm [4,8], even if structural parameters (mainly, atomic positions and thermal factors) may be known and therefore considered as constants. It is also possible to use a WPPF without modelling the diffracted intensity by means of a structural model, but as a fitting parameter. This approach is particularly effective to study lattice defects and cell parameters in single-phase and multiphase materials [5][1].

Most methods proposed so far are based on the modelling of experimental data with analytical functions, like Voigt (convolution of a Gaussian (G) and a Lorentzian (or Cauchy) (C) curve [11]), pseudo-Voigt (pV) (weighted average of G and C, with mixing factor η: $(1-\eta)G+\eta C$ [12]) or Pearson VII (a modified C curve [13]), just to cite the most common ones [14]. Using an analytical function to model a diffraction profile is certainly an arbitrary choice; however, this approach has become increasingly popular for practical reasons, as it permits a fast and efficient extraction of information from the experimental pattern, and is a simple way to study broad and overlapped diffraction profiles. Experience has also shown that, frequently, analytical functions reproduce quite well real diffraction data (*e.g.*, see [15]). Therefore this approach can be considered as partially legitimate; however, limits and possible artefacts due to the use of analytical functions to fit experimental data (which limit possible shapes of the modelled profile) should always be borne in mind.

Several approaches have been proposed to extract information (i–v) *after* WPPF, using the refined profile data (like position, width and shape) [5]; we can consider these as *a posteriori* techniques, whose reliability is strongly

[a] e-mail: paolo.scardi@ing.unitn.it

[1] Some authors attribute to Pawley [9,10] the introduction of WPPF, even if considerable changes have been made to the original approach; for instance, see [1,5].

limited by the quality of the WPPF itself. The statistical weight of the intensity, which is an important piece of information, is not directly related to the estimated errors of structural and defect parameters. In spite of that, this approach is probably the most used at present, because is quite straightforward and can be used in principle for any crystalline phase without a knowledge of structural data.

A different procedure has been recently proposed for fcc materials by some of the authors [3]. The line profile parameters connected with domain size, faulting and lattice distortions (due to dislocations) where directly included in a least square algorithm for WPPF based on the use of pV profile functions. Applications to different inorganic materials was successful, and provided an effective means to account for line broadening anisotropy, *i.e.*, changes in peak shape and width for different (hkl), additional to the effect of the reflection order on lattice distortions. The main limit was in the oversimplified size broadening model, which was rather arbitrary and inaccurate to fit high angle reflections. In the present work we propose an extension of the cited approach, based on much more general assumptions regarding domain size effects, and a fast and effective least squares algorithm that can easily be incorporated in WPPF or Rietveld programs.

2 Methodology

2.1 Introductory remarks

Diffraction profiles from polycrystalline materials can be written as Fourier integrals, whose coefficients are connected with the various possible sources of line broadening, which typically include an instrumental component and sample-dependent physical effects [16]. For a given set of planes with Miller indices $\{hkl\}$, the diffracted intensity is conveniently represented in the reciprocal lattice, introducing the modulus of the diffraction vector, $d^* = 2\sin\theta/\lambda$, where θ is the diffraction angle and λ is the wavelength. If profiles are symmetrical, the diffracted intensity can be expressed by a cosine Fourier integral (analogous expressions should be written for all the spectral components of the radiation employed),

$$I(d^*) = k(d^*)\int_0^\infty A(L)\cos\left[2\pi L(d^* - d^*_{\mathrm{B}} - \delta)\right]\mathrm{d}L \quad (1)$$

where d^*_{B} is the value of d^* in Bragg condition, in absence of lattice defects, and δ is the shift due to faulting. $k(d^*)$ accounts for all effects that are constant for a given peak, or are known functions of d^* (*e.g.*, diffraction geometry, Lorentz-polarisation factor, multiplicity, $|F|^2$, etc. [17]). The variable (L) in the integral is the Fourier length, which is a length in the real space along the direction of the diffraction vector ($L = n/d^*$, where n is an integer).

Instrumental features as well as some types of lattice defects can produce asymmetric profiles [17–20]; in this work we deal with the asymmetry due to twin faults, which will be introduced later. A general approach for asymmetric profiles involves an additional sine term in (1) [21]. In the following, however, we will only consider cosine terms, so we will refer to them as Fourier coefficients, omitting the adjective “cosine”.

The Fourier coefficients, $A(L)$, carry the information on peak shape and width and can be written as:

$$A(L) = T^{\mathrm{IP}}(L)A^{\mathrm{S,F}}(L)A^{\mathrm{D}}(L). \quad (2)$$

The three terms in (2) represent the effect of instrumental profile ($T^{\mathrm{IP}}(L)$), crystallite size and stacking faults ($A^{\mathrm{S,F}}(L)$), and lattice distortions ($A^{\mathrm{D}}(L)$). Expressions for instrumental, size/faulting and distortion terms can be written according to suitable models; in this work they are based on the following hypotheses:

- Studied materials have fcc structure and no appreciable texture is present; extension to bcc and hcp is straightforward. The proposed approach, in principle, can be further extended to any symmetry, provided that suitable relations for size/faulting and distortion terms in (2) are available.
- Crystalline domains are spherical, with a lognormal distribution of diameters. This assumption is quite general, and seems to be appropriate in several cases, including materials as different as finely dispersed ceramics and highly deformed metals (see [6] and Refs. therein). The corresponding size-broadening effect is isotropic (*i.e.*, independent of (hkl)), and can be modelled in terms of lognormal mean (γ) and variance (ω). The model can be extended to consider different crystallite shapes and size distributions.
- The contribution of faulting is written according to Warren's theory [17]. Modelling is limited to low faulting probabilities, and an average profile is calculated for each family of planes $\{hkl\}$. This is an approximation, since faulting should be treated by separating the diffraction signal from a $\{hkl\}$ family into profile sub-components with different hkl. However, the complexity of this operation is beyond the limits of the proposed model.

2.2 Instrumental broadening

The instrumental profile (IP) is assumed to be symmetrical, condition easily obtained by using suitable diffraction optics [22]; in general, since we are mostly concerned with broadened profiles, where the instrument contribution is not critical, the assumption of a symmetrical IP is appropriate. Under these conditions, the IP can be analytically modelled for a wide portion of the diffraction pattern by means of Voigt or pseudo-Voigt curves [22,23]. If we consider a pV, the Fourier transform can be written as:

$$T^{\mathrm{IP}}_{pV}(L) = (1-k)\exp(-\pi\beta^2_{pV,G}L^2) + k\exp(-2\beta_{pV,C}L) \quad (3)$$

where $k = \eta\beta_C/\beta$, and β, β_C and β_G are integral breadths (peak area/maximum intensity) of the pV and

its Lorentzian and Gaussian components, respectively. By modelling the experimental pattern of a suitable profile standard [23], one can obtain a parametric description of the IP and its transform, $T_{pV}^{\mathrm{IP}}(L)$ [3].

2.3 Effect of faulting and domain size

Planar defects, which are assumed to lay in the (111) planes, can be described in terms of deformation and twin faulting probabilities (α and β, respectively). The size (A^{S}) and faulting (A^{F}) coefficients can then be separated as:

$$A^{\mathrm{S,F}}(L) = A^{\mathrm{S}}(L) A_{hkl}^{\mathrm{F}}(L; \alpha, \beta). \quad (4)$$

Size coefficients can be calculated from the column length distribution, $p(L)$. If we assume to divide each spherical grain in columns of cells along the direction of the diffraction vector, $p(L)$ is the distribution of distances between cells inside columns [17]. Such a distribution can be calculated for spheres whose diameters are distributed according to a lognormal ($p(D)$):

$$p(D) = \frac{1}{D\omega\sqrt{2\pi}} \exp\left[-\frac{(\ln D - \gamma)^2}{2\omega^2}\right] \cdot \quad (5)$$

To obtain $p(L)$, with need to consider the distribution for a single sphere, $p_{\mathrm{s}}(L; D) = 2L/D^2$ [24], weighted over the lognormal distribution (5):

$$p(L) \propto \int_{|L|}^{\infty} p_{\mathrm{s}}(L; D) g(D) \mathrm{d}D. \quad (6)$$

Solving the integral (6), and after suitable normalisation, the column length distribution is

$$p(L) = L \exp(-2\gamma - 2\omega^2) \mathrm{erfc}\left(\frac{\ln L - \gamma}{\sqrt{2}\omega}\right) \cdot \quad (7)$$

The size Fourier coefficients, according to Bertaut [17,25], can be calculated as:

$$A^{\mathrm{s}}(L) = \frac{1}{\langle L \rangle} \int_{L}^{\infty} (L' - L) p(L') \mathrm{d}L' \quad (8)$$

where $\langle L \rangle$ is the mean column length [17]. The integration of (8) gives an analytical expression for $A^{\mathrm{s}}(L; \gamma, \omega)$, which according to our hypotheses is independent of (hkl); therefore, size Fourier coefficients for all diffraction profiles depend on γ and ω only.

According to Warren [17], the faulting coefficients can be written as:

$$A_{hkl}^{\mathrm{F}}(L) = \frac{1}{m} \sum_{m} Z^{\left| L d_{\mathrm{B}}^{*} \frac{L_0}{h_0^2} \sigma_{L_0} \right|} \quad (9)$$

where $L_0/h_0^2 = (h+k+l)/(h^2+k^2+l^2)$,

$$\sigma_{L_0} = \begin{cases} +1 & \text{for } L_0 = 3N+1 \\ 0 & \text{for } L_0 = 3N \qquad N = 0, \pm 1, \pm 2, ... \\ -1 & \text{for } L_0 = 3N-1 \end{cases} \quad (10)$$

and

$$Z = (1 - 3\alpha - 2\beta)^{1/2}. \quad (11)$$

The $\sum_m$ (where m is the multiplicity) is intended as a sum over all the (hkl) components belonging to a $\{hkl\}$ plane family. As can be seen from (9) and (10), the number of independent components is less than m; in fact, only the value of L_0 and the selection rules of (10) are important (maximum number of independent components is four). Faulting is also responsible for a hkl-dependent shift in the diffraction peak centroid proportional to α [2]:

$$\delta_{hkl} = \frac{1}{m} \sum_{m} d_{\mathrm{B}}^{*} \frac{\sqrt{3}\alpha}{4\pi} \frac{L_0}{h_0^2} \sigma_{L_0}. \quad (12)$$

In conclusion, the contribution of faulting to line broadening and peak position can be written in terms of faulting probabilities (α and β), and is different for the various (hkl) reflections.

2.4 Lattice distortions due to dislocations

The calculation of the last term in (2) ($A^{\mathrm{D}}(L)$) requires some assumption on the nature of the defects producing the lattice distortion. Dislocations are frequently responsible for lattice distortion (usually referred to as *microstrain*) in a wide variety of materials. The corresponding line broadening effect, which is anisotropic, can be described in terms of dislocation density (ρ) and outer cut-off radius (R_{e}) (or similar characteristic distances [27]); following Wilkens [28,29] and van Berkum [30], the following expression can be written for the distortion Fourier coefficients:

$$A^{\mathrm{D}}(L) = \exp\left[-\frac{1}{2}\pi |b|^2 \overline{C}_{hkl} \rho d_{hkl}^{*2} L^2 f^{*}(L/R_{\mathrm{e}})\right] \quad (13)$$

where **b** is the Burgers vector (the slip system in fcc structures is $\{111\}\langle 110 \rangle$, for which $|b| = a_0/\sqrt{2}$, where a_0 is the lattice parameter) and $f^{*}(L/R_{\mathrm{e}})$ is a known function [30]. Following the theory of Wilkens, a higher order term can be added to the exponent in (13), whose leading term is of the type: $g(L^4)\rho^2 \overline{C}_{hkl}^2 d_{hkl}^{*4}$; the expression of $g(L^4)$ can be worked out from references [28–30]. The weight of the higher order term is considerably less than that proportional to $L^2 f^{*}$ in (13), and its importance is appreciated only for high diffraction angles (high d^{*}) and around the peak top, where large L are important.

$\overline{C}_{hkl}$ is the average contrast factor, which accounts for the anisotropy of the dislocation strain field that is responsible for the anisotropic line broadening effect (actually,

[2] Expressions given by Warren were obtained for low faulting probabilities; for higher probabilities suitable relations recently derived by Velterop *et al.* [26] should be used. On the other hand, the present approach is not suitable for high faulting probabilities, since, as discussed previously (see Sect. 2.1) profile sub-components should be calculated separately.

according to the different dislocation models, part of the dependence on (hkl) is carried by R_e [28]; in the present work we consider R_e as a fitting parameter independent of (hkl) [29]). As originally proposed several years ago by Stokes and Wilson [31], line broadening anisotropy can be introduced by assuming a linear dependence of the microstrain on the orientational parameter H (also referred to as Γ [32]); this corresponds to write the contrast factor for the cubic system as [3,33]:

$$\overline{C}_{hkl} = \overline{C}_{h00}(1 + qH) = \overline{C}_{h00}\left[1 + q\frac{h^2k^2 + h^2l^2 + k^2l^2}{(h^2 + k^2 + l^2)^2}\right] \tag{14}$$

where $\overline{C}_{h00}$ and q can be calculated from the elastic constants of the material (c_{ij} or s_{ij}) for different types of dislocations [34]. As shown recently by Ungár *et al.* [33], $\overline{C}_{h00}$ and q for screw and edge dislocations can be conveniently expressed in a parametric form as a function of the elastic constants. If the elastic constants are known, the average contrast factor can be calculated, and $A^{\mathrm{D}}(L)$ depends on ρ and R_e only. Additionally, q can be refined in order to adjust the modelling result for the appropriate screw/edge character of the dislocations [3].

2.5 WPPF algorithm

From the discussion above it is possible to write an analytical expression for $A(L)$ in (2). In order to model the diffraction peaks in the experimental pattern, we assume profiles to be Voigtians. This is clearly an arbitrary hypothesis, since experimental profiles can in principle have any shape; however, much of the work in the recent literature has shown that Voigt curves are appropriate to model many observed patterns from polycrystalline samples [15]. As we will see in the following, the advantage of this hypothesis is the possibility to develop a rather simple and fast algorithm to model the line broadening effects of (2). In principle, however, the present approach could also be used with a different analytical profile function (*e.g.*, a pV or a Pearson VII).

The Fourier transform of a Voigtian is a simple two-parameter expression:

$$T_V(L) = \exp(-\pi\beta_{V,G}^2L^2 - 2\beta_{V,C}L) \tag{15}$$

where $\beta_{V,G}$ and $\beta_{V,C}$ are the integral breadths of the Gaussian and Lorentzian components (that should not be confused with the corresponding parameters for a pV function [11,15]).

For each (hkl) diffraction profile, the basic equation for the whole powder pattern fitting can be written as:

$$\sum_L w_L\left[T_V(L) - A(L)\right]^2 = \text{min.}, \tag{16}$$

where w_L is a weight. In practice, a least squares algorithm is used to fit the Fourier transform of a Voigtian profile to (2); the fitting of the experimental data is therefore carried out by optimising the values of $\beta_{V,G}$ and $\beta_{V,C}$ for each diffraction profile, in terms of the fitting parameters connected to size/faulting and distortion effects: $\alpha, \beta, \gamma, \omega, \rho, R_e, (\overline{C}_{h00})$ and q.

As a weight function in (16) we can use $w_L = A(L)$; in this way we can give more weight to the information carried by the tails of profiles (low L values) with respect to the peak top, which is consistent with the statistical weight in the experimental pattern. Formally, the upper limit in the summation of (16) is infinity; from a practical point of view, the calculation can be stopped when $A(L)$ falls below a given threshold (*e.g.* 10^{-3}). Most importantly, we note that (16) can be solved analytically, which means in a very fast and efficient way in terms of computation time. This also provides an efficient way to test the validity of a given model for line broadening, expressed by (2).

2.6 Profile asymmetry due to twin faults

Finally, we should consider that twin faults are cause of asymmetry in some profiles. As indicated above, a rigorous model would require the introduction of sine terms in (1). In the proposed approach we adopt a simplified model, always in the limit of low faulting probabilities, which is essentially the same as that used by Scardi and Leoni [3], based on the use of split profile function; the basic difference is that we now use split Voigt curves (Voigtians with different integral widths for low and high angle tails (β_{low} and β_{high}, respectively)) instead of split pV curves [3].

According to the Warren theory, a reasonable estimate of asymmetry can be obtained considering that the difference between β_{high} and β_{low} is proportional to $\beta\sum_m \frac{L_0}{|L_0|}\sigma_{L_0}$. Also in this case, limitations expressed in Section 2.1 and footnote 2 apply. Details on the algorithm to include asymmetry with split profile functions are reported in the cited references [3,21].

3 Experimental

X-ray diffraction (XRD) patterns were collected using a Rigaku PMG-VH diffractometer, adopting the conventional Bragg-Brentano geometry. Goniometer optics included a graphite curved-crystal analyser in the diffracted beam and narrow slits (Soller = 2°; DS = 1/2°; Soller = 2°; RS = 0.15 mm, in the order, from source to secondary circle (graphite analyser) and scintillation counter).

The IP was measured over a wide angular range (25–150°) from the experimental pattern of a suitable KCl profile standard [22,23], and no asymmetry was observed within the accuracy of pV curve fitting. The procedure also permitted an optimisation of the observed ratio and angular distance between the spectral components of the Cu Kα radiation.

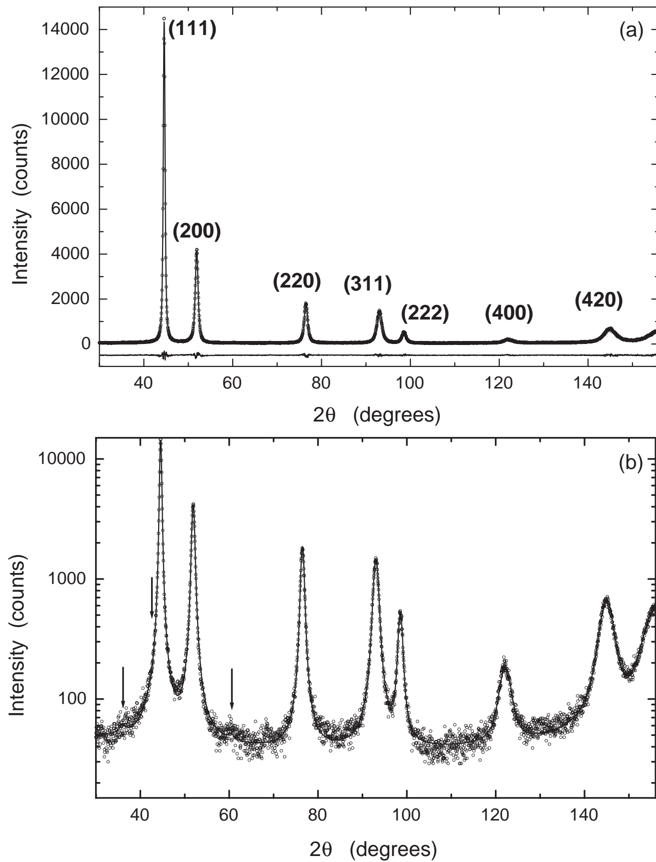

Fig. 1. Results of Whole Powder Pattern Fitting for a Ni sample ball milled for 24 hours. Experimental (circle) and modelled (line) patterns are reported together with their difference (residual, below) in linear (a) and logarithmic (b) scale. Arrows indicate the position of strong lines of the native oxide (NiO).

4 Results and discussion

The method described so far was applied to two different inorganic polycrystalline materials. The first example is a Ni powder ball milled for 24 hours. Figure 1a shows the experimental and modelled patterns with their difference (residual). The quality of the modelling in the tail region can be better appreciated in the log scale plot (Fig. 1b), where it is also possible to note the little contribution from Ni oxide (NiO, Bunsenite), which was included in the modelling algorithm. Refined parameters for the ball milled Ni sample are reported in Table 1.

We included the Wilkens' parameter ($\mu = R_e\sqrt{\rho}$), which can be related to the distribution of dislocations and their interaction [29]; the refined value is comparable to that from previous studies on similar materials [3,33], within the limits of validity of (13) (*cf.* Wilkens [29]) .

Line broadening anisotropy is quite evident, and according to our results is mostly due to a high dislocation density; from the refined value of q, we can judge that the dislocation character is not far from 50% edge - 50% screw. Profiles are reasonably symmetric, and consequently twin faults are absent, whereas a low fraction of deformation faults is present; under these conditions, approximations

Table 1. Results of WPPF: lattice parameter (a_0), lognormal mean (γ), variance (ω) and mean grain diameter ($\langle D\rangle$); average contrast factor along for ($h00$) ($\overline{C}_{h00}$) and slope in (12) (q); Wilkens' parameter (μ) and dislocation density (ρ); deformation fault (α) and twin fault (β) probabilities; statistical quality indices of fitting: R_{w}, R_{exp}, GoF [4].

	Ni powder		Li, Mn spinel [35]
	As received	24h ball milling	treated at 800 °C
a_0 (nm)	0.35228(1)	0.35242(1)	0.824544(5)
γ	4.10(2)	2.95(2)	2.0(5)
ω	0.10(3)	0.39(1)	0.99(6)
$\langle D\rangle$ (nm)	61(2)	20.1(5)	12(1)
$\overline{C}_{h00}$	0.266[a]	0.266[a]	0.3[a]
q	1.81[a]	1.88(3)	2.55(4)
μ	~2	1.5(1)	0.9(2)
$\rho(\times 10^{15})$ m^{-2}	0.58(1)	10.8(5)	0.22(2)
α (%)	0	0.68(2)	0
β (%)	0	0	0
R_{wp} (%)	9.40	7.34	13.90
R_{exp} (%)	6.29	6.45	11.99
GoF	1.49	1.14	1.16

[a] fixed value, calculated for 50% screw - 50% edge dislocations [3,33].

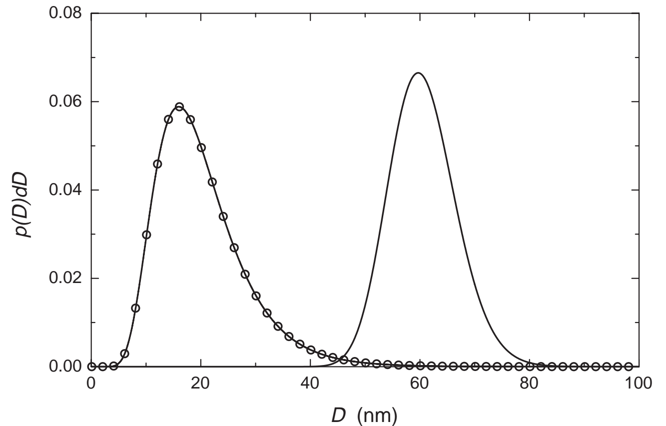

Fig. 2. Distribution of diameters of spherical grains for ball milled (line-circle) and as received (line) Ni powder.

on line broadening and asymmetry due to faulting should be justified.

It is interesting to compare these results with those for the starting powder, which was composed of spherical particles with diameters of the order of several microns. As shown in Table 1, the concentration of defects is much lower in the as received powder, toward the limits of sensitivity of the method; for this reason q was not refined, and Wilkens' parameter is affected by a large error. The main source of line broadening in the as received powder is due to crystallite size; quite obviously metal particles were not single-crystals (a result confirmed by a preliminary TEM investigation). Figure 2 shows a comparison between the lognormal distribution of sphere diameters for

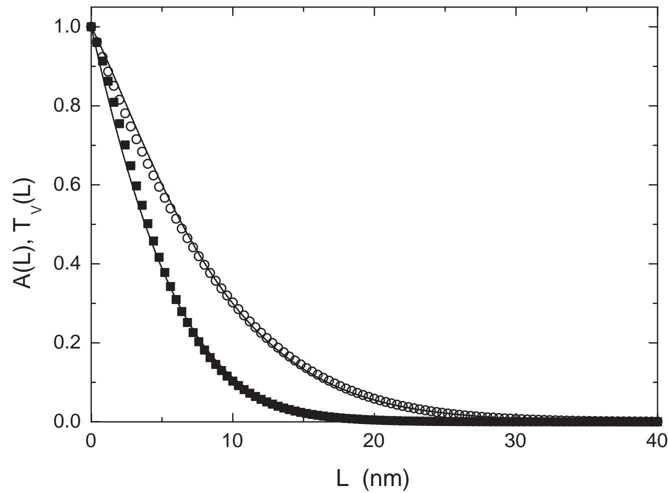

Fig. 3. Cosine Fourier coefficients for the (111) (○) and (200) (■) profiles of Figure 1, calculated according to the size/faulting/distortion model of (2) ($A(L)$, symbols) and for the corresponding Voigt curves ($T_V(L)$, line) according to (15).

the two studied samples. Before ball milling the average diameter is peaked about 60 nm, with a quite narrow distribution: under these conditions ($\omega \approx 0$, see Tab. 1) the distribution is not far from a Gaussian. After ball milling the distribution shifts to smaller size and shows a higher variance, but still preserves a tail toward the values of the starting distribution. Finally we can note the increase in lattice parameter due to lattice defect incorporation after ball milling.

Figure 3 shows the Fourier coefficients (2) compared with those of the refined Voigtian profiles (given by (15)) for the (111) and (200) reflections. The agreement between the size/faulting/distortion model and Voigtian transform is good; in addition, a comparison between the trends for (111) and (200) clearly demonstrates the strong line broadening anisotropy. This last feature is better appreciated in the so-called Warren-Averbach plot [17], where the logarithm of the Fourier coefficients (corrected for the IP component) is plotted against d^{*^2}. As shown in Figure 4a, there is a large scatter of the data caused by the anisotropic line broadening due to dislocations [3,19]. The effectiveness of the model (and (13) in particular) can be judged from the linearity of the trend in Figure 4b, where the same Fourier coefficients are plotted as a function of $d^{*^2}\overline{C}_{hkl}$.

It is worth underlining that the results of Figure 4b were obtained by the proposed WPPF method, *i.e.*, by a simultaneous refinement of the size/faulting/distortion parameters directly performed on the observed data. This is a major improvement in Line Profile Analysis (LPA), where conventional approaches mostly rely on *a posteriori* methods (*cf.* Sect. 1), that can be biased by the model used to extract profile information from raw data. For example, limits of conventional LPA methods are evident in the presence of peak overlapping, which is always ob-

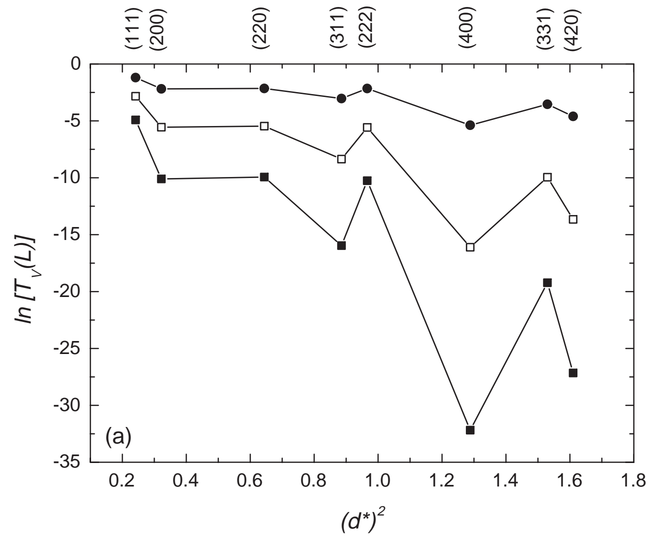

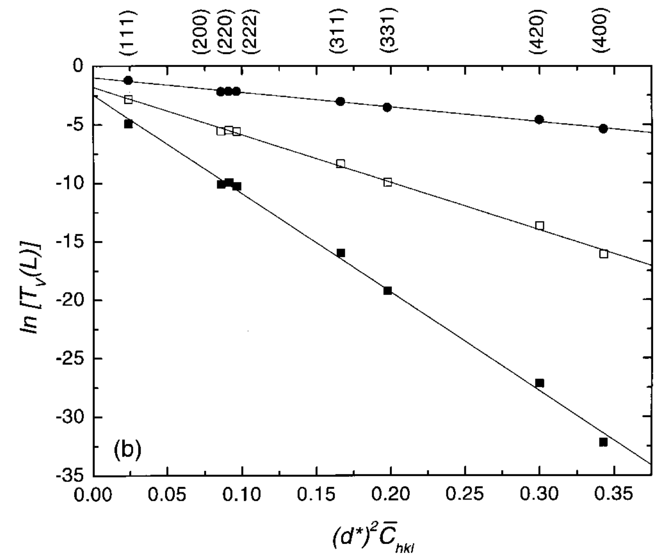

Fig. 4. Conventional (a) and modified (b) Warren-Averbach plot for the ball milled Ni sample of Figure 1 (see text): L = 10 (●), L = 20 (□) and L = 30 (■) nm.

served in cases of practical interest, when broad profiles are measured.

As a further example we considered a Li,Mn spinel sample. The studied system, obtained from a crystallisation (800 °C) of an amorphous gel [35], is a finely dispersed ceramic powder for which the assumption of equiaxial grains with a lognormal size distribution is expected to be appropriate [6]. Previous studies on similar samples [3,36,37] indicated the presence of a marked line broadening anisotropy, reasonably attributed to dislocations.

Figure 5 shows the results of WPPF; defects parameters and quality indices are reported in Table 1. In this case 35 profiles were modelled simultaneously with an excellent agreement between observed and modelled patterns. The log scale plot of Figure 5b highlights the quality

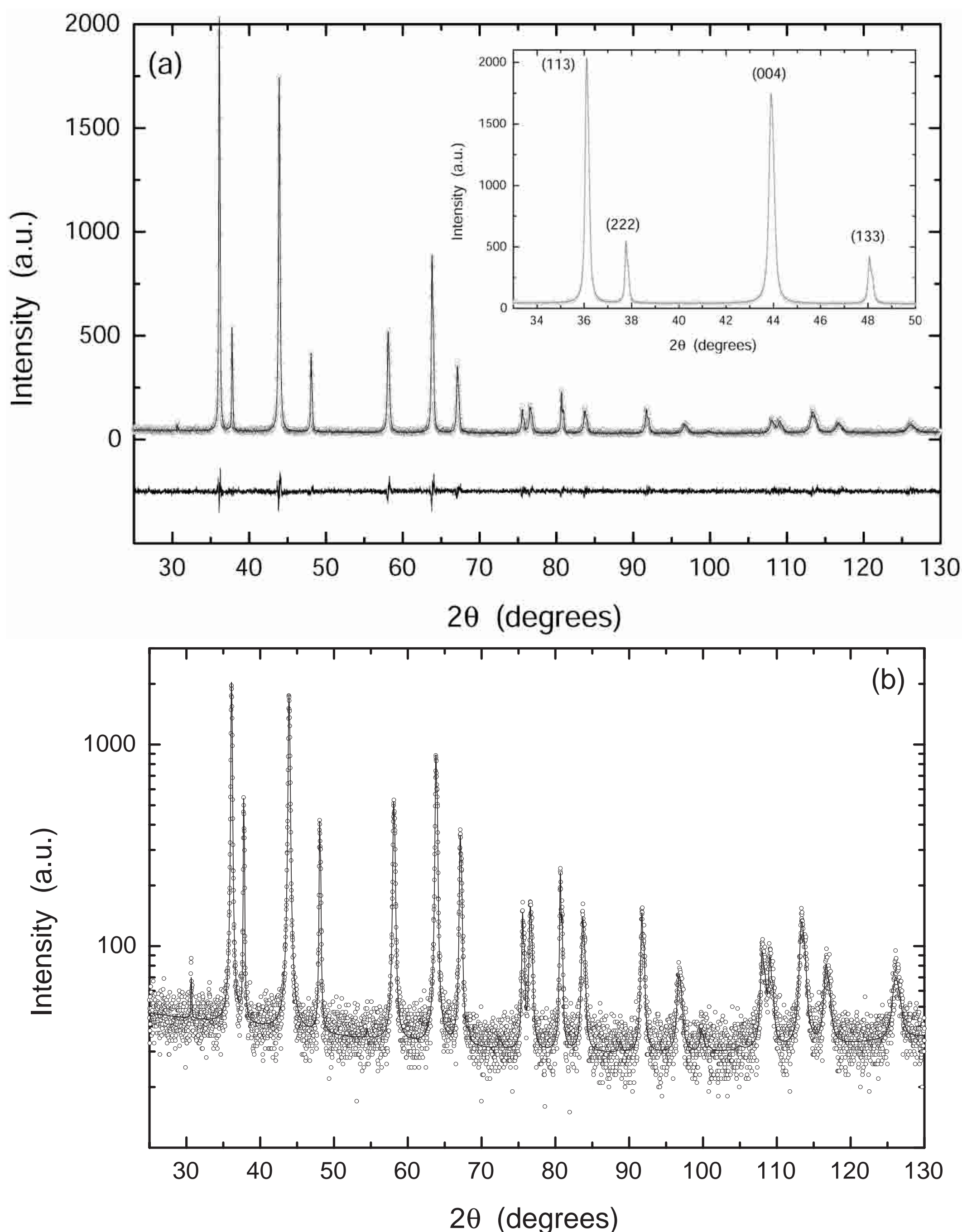

Fig. 5. Results of WPPF for a Li,Mn spinel sample. Graphical output in linear (a) and logarithmic (b) scale.

of peak tail fitting, whereas the inset of Figure 5a shows a detail of the line broadening anisotropy effect in the low 2θ range.

The results discussed so far demonstrate the effectiveness of the proposed method, and the quality and detail of information attainable. The devised algorithm is simple, and leads to a convergence in a few least squares iterations. Limits in the modelling that need to be improved concern faulting; however, possible inadequacies of the present approach are likely to be reduced when size and distortion effects are prevalent sources of line broadening. The major fault in Warren's theory, concerning the average over m (see (9, 12) and footnote 2), produces significant deviations from the correct result when faulting is the main source of broadening, a situation that is likely to happen in a few cases [26]; examples illustrated in this work seems not to fall in this category. In any case, splitting each reflection of a $\{hkl\}$ plane family into sub-components with different width, asymmetry and shift is a necessary development [21].

Another important issue concerns avoiding the use of analytical functions to model the pattern. We have already

underlined that this is an arbitrary hypothesis, whose consequences on the reliability of the results are not easily controlled, and are certainly sample-dependent. For instance, the limitation of using Voigt profile functions is apparent from both curves in Figure 3 for small L: a small but non negligible discrepancy can be observed. As recently stated by Langford *et al.* [6], in finely dispersed systems (like ceramic powders and deformed metals) there may well be an appreciable systematic error in $\langle D \rangle$ due to deviation of the Voigt profile shape from the profile function produced by a real system; in our case, deviations are with respect to (5).

5 Conclusion

A new method of whole powder pattern fitting based on the use of Voigt functions has been described and tested on two different cases of study. The algorithm proved to be fast and effective in reproducing the experimental pattern of fcc materials, and can in principle be adapted to other structures within WPPF or Rietveld programs.

The major advancement with respect to previous approaches is that all the main components of sample-related line broadening are considered on the basis of well-defined physical models:

- size broadening is connected with the column length distribution in a system of spherical grains, whose diameters are distributed according to a lognormal (in principle, different grain shapes and distributions can be considered);
- planar defects are dealt with in terms of probability of finding twin and stacking faults in the (111) planes, with the assumption of low defect concentrations;
- lattice distortions are attributed to dislocations, whose anisotropic strain field is considered in terms of the average contrast factor, dislocation density and outer cut-off radius.

The authors wish to thank J.I. Langford for helpful discussion and suggestions, and S. Setti for assistance in laboratory measurements.

References

1. J.I. Langford, D. Louër, Rep. Prog. Phys. **59**, 1 (1996).
2. P. Scardi, in *Defect and Microstructure Analysis by Diffraction*, edited by R.L. Snyder, J. Fiala, H.-J. Bunge (Oxford University Press, Oxford, 1999), pp. 570–596.
3. P. Scardi, M. Leoni, J. Appl. Cryst. **32**, 671 (1999).
4. R.A. Young, *The Rietveld Method* (Oxford University Press, Oxford, 1993).
5. Y.H. Dong, P. Scardi, J. Appl. Cryst. **33**, 184 (2000).
6. J.I. Langford, D. Louër, P. Scardi, J. Appl. Cryst. **33**, 964 (2000).
7. M. Järvinen, in *Defect and Microstructure Analysis by Diffraction*, edited by R.L. Snyder, J. Fiala, H.-J. Bunge (Oxford University Press, Oxford, 1999), pp. 556–569; V. Honkimäki, P. Suortti, *ibidem*, pp. 41–58.
8. H.M. Rietveld, J. Appl. Cryst. **2**, 65 (1969).
9. H. Toraya, in *The Rietveld Method*, edited by R.A. Young (Oxford University Press, Oxford, 1993), pp. 254–275.
10. G.S. Pawley, J. Appl. Cryst. **14**, 357 (1981).
11. J.I. Langford, J. Appl. Cryst. **11**, 10 (1978).
12. G.K. Wertheim, M.A. Butler, K.W. West, D.N.E. Buchanan, Rev. Sci. Instrum. **11**, 1369 (1974).
13. M.M. Hall, V.G. Veeraraghavan, H. Rubin, P.G. Winchell, J. Appl. Cryst. **10**, 66 (1977).
14. R.A. Young, D.B. Wiles, J. Appl. Cryst. **15**, 430 (1982).
15. J.I. Langford, in *Defect and Microstructure Analysis by Diffraction*, edited by R.L. Snyder, J. Fiala, H.-J. Bunge (Oxford University Press, Oxford, 1999), pp. 59–81.
16. H.P. Klug, L.E. Alexander, *X-ray Diffraction Procedures*, 2nd edn. (John Wiley and Sons, New York, 1974).
17. B.E. Warren, *X-ray Diffraction* (Addison Wesley, New York, 1969).
18. R.L. Snyder, in *The Rietveld Method*, edited by R.A. Young (Oxford University Press, Oxford, 1993), pp. 111–131.
19. T. Ungár, in *Defect and Microstructure Analysis by Diffraction*, edited by R.L. Snyder, J. Fiala, H.-J. Bunge (Oxford University Press, Oxford, 1999), pp. 165–199.
20. A.C. Nunes, D. Lin, J. Appl. Cryst. **28**, 274 (1995).
21. P. Scardi, M. Leoni, Y.H. Dong, Mat. Sci. Forum (2000) in press; P. Scardi, M. Leoni, Y.H. Dong (in preparation).
22. P. Scardi, L. Lutterotti, P. Maistrelli, Powder Diffraction **9**, 180 (1994).
23. M. Leoni, P. Scardi, J.I. Langford, Powder Diffraction **13**, 210 (1998).
24. W.L. Smith, J. Appl. Cryst. **9**, 187 (1976).
25. F. Bertaut, C.R. Acad. Sci. Paris **228**, 492 (1949).
26. L. Velterop, R. Delhez, Th.H. de Keijser, E.J. Mittemeijer, D. Reefman, J. Appl. Cryst. **33**, 296 (2000).
27. M.A. Krivoglaz, O.V. Martynenko, K.P. Ryaboshapka, Phys. Met. Metall. **55**, 1 (1983).
28. M. Wilkens, in *Fundamental Aspects of Dislocation Theory*, edited by J.A. Simmons, R. de Wit, R. Bullough (Nat. Bur. Stand., (US) Spec. Publ. No 317, Washington, DC. USA, 1970), Vol. II, pp. 1195–1221.
29. M. Wilkens, Phys. Stat. Sol. (a) **2**, 359 (1970).
30. J.G.M. van Berkum, Ph.D. thesis, Delft University of Technology, 1994.
31. A.R. Stokes, A.J.C. Wilson, Proc. Phys. Soc. London **56**, 174 (1944).
32. V. Hauk, *Structural and Residual stress Analysis by Nondestructive Methods* (Elsevier, Amsterdam, 1997); I.C. Noyan, J.B. Cohen, *Residual Stress* (Springer-Verlag, New York, 1987).
33. T. Ungár, I. Dragomir, A. Reves, A. Borbely, J. Appl. Cryst. **32**, 992 (1999).
34. M. Wilkens, Phys. Stat. Sol. (a) **104**, K1 (1987); R. Kuzel Jr., P. Klimanek, J. Appl. Cryst. **21**, 363 (1988).
35. V. Massarotti *et al.*, unpublished results (2000).
36. V. Massarotti, M. Bini, D. Capsoni, P. Scardi, M. Leoni, Mat. Sci. Forum **278-281**, 820 (1998).
37. V. Massarotti, D. Capsoni, M. Bini, P. Scardi, M. Leoni, V. Baron, H. Berg, J. Appl. Cryst. **32**, 1186 (1999).